Kinetic Coupled with UV Spectral Evidence for Near-Irreversible Nonionic Micellar Binding of *N*-Benzylphthalimide under the Typical Reaction Conditions: An Observation Against a Major Assumption of the Pseudophase Micellar Model

May Ye Cheong, Azhar Ariffin, and M. Niyaz Khan*

Department of Chemistry, Faculty of Science, University of Malaya, 50603 Kuala Lumpur, Malaysia

Received: May 23, 2007; In Final Form: August 7, 2007

Pseudo-first-order rate constants (k_{obs}) for alkaline hydrolysis of *N*-benzylphthalimide (**1**) show a nonlinear decrease with the increase in $[C_mE_n]_T$ (total concentration of Brij 58, $m = 16$, $n = 20$ and Brij 56, $m = 16$, $n = 10$) at constant [CH_3CN] and [NaOH]. These nonionic micellar effects, within the certain typical reaction conditions, have been explained in terms of the pseudophase micellar (PM) model. The values of micellar binding constants (K_S) of **1** are 1.04×10^3 M^{-1} (at 1.0×10^{-3} M NaOH) and 1.08×10^3 M^{-1} (at 2.0×10^{-3} M NaOH) for $C_{16}E_{20}$ as well as 600 M^{-1} (at 7.6×10^{-4} M NaOH) and 670 M^{-1} (at 1.0×10^{-3} M NaOH) for $C_{16}E_{10}$ micelles. The pseudo-first-order rate constants (k_M) for hydrolysis of **1** in $C_{16}E_{20}$ micellar pseudophase are ~90-fold smaller than those (k_W) in water phase. The values of k_M for hydrolysis of **1** in $C_{16}E_{10}$ micelles are almost zero. Kinetic coupled with UV spectral data reveals significant irreversible nonionic micellar binding of **1** molecules in the micellar environment of nearly zero hydroxide ion concentration at ≥0.14 M $C_{16}E_{20}$ and 1.0×10^{-3} M NaOH while such observations could not be detected at ≤0.17 M $C_{16}E_{20}$ and 2.0×10^{-3} M NaOH. Significantly, such irreversible $C_{16}E_{10}$ micellar binding of **1** molecules could be detected at 8.8×10^{-2} M $C_{16}E_{10}$ and 1.0×10^{-3} M NaOH as well as at ≥3×10^{-3} M $C_{16}E_{10}$ and 7.6×10^{-4} M NaOH, while the rate of hydrolysis of **1** is completely ceased at ≥0.05 M $C_{16}E_{10}$ and 7.6×10^{-4} M NaOH. The rate of hydrolysis of **1** at 5.0×10^{-2} and 8.8×10^{-2} M $C_{16}E_{10}$ and 1.0×10^{-3} M NaOH reveals the formation of presumably phthalic anhydride, whereas such observation was not observed in the $C_{16}E_{20}$ micellar system under similar experimental conditions.

Introduction

The classical pseudophase micellar (PM) model and its various extended forms contain a basic and common assumption that the micellar reaction environment/solubilization site constitutes a uniform and homogeneous medium.[1] But indirect experimental evidence is making the fact increasingly clearer that the micellar reaction/solubilization environment is not completely homogeneous in terms of polarity/dielectric constant, water concentration, water structure, viscosity, and ionic strength (for ionic micelles only).[2] But, it seems that the changes in these physicochemical properties with change in distance from the exterior to deep interior of the micelle are gradual and continuous.[3] Perhaps because of this micellar characteristic, the multiple micellar pseudophase (MMP) model of Davies led to the kinetic equation similar (in form) to one derived based upon the classical two-state PM model with a modified definition of micellar binding constant of reactants and rate constant for micellar-mediated reaction.[4] There appears to be no report in the literature against this generalization. However, irreversible micellar portioning of two different reactants in terms of hydrophilicity has been recently observed at larger than a typical value of $[C_{12}E_{23}]_T$/[NaOH] (= R_t) in $C_{12}E_{23}$ micellar-mediated alkaline hydrolysis of phthalimide,[5] phenyl benzoate (PB),[6] and phenyl salicylate (PSH)[6] as shown in reaction Scheme 1. These observations cannot be ascribed to a shielding effect of micelles because the observed data, obtained at R (= $[C_{12}E_{23}]_T$/[NaOH]) values below the typical R_t value, have been explained in terms of the PM model while shielding the effect of the micelles is not expected to display such micellar-mediated reaction characteristics. The shielding effect of micelles depends only upon the difference of the hydrophobicity of the two different reactant molecules, and it should be independent of the nature of micelle-forming surfactants. Irreversible micellar trapping of PSH[7] and PB[8] could not be detected in pH-independent hydrolysis and hydrazinolysis of PSH in the presence of anionic micelles and alkaline hydrolysis of PB in the presence of $C_{16}E_{20}$, micelles. These observations are not in favor of a shielding effect as the cause of the irreversible trapping of PSH and PB at R values $> R_t$.[5]

SCHEME 1

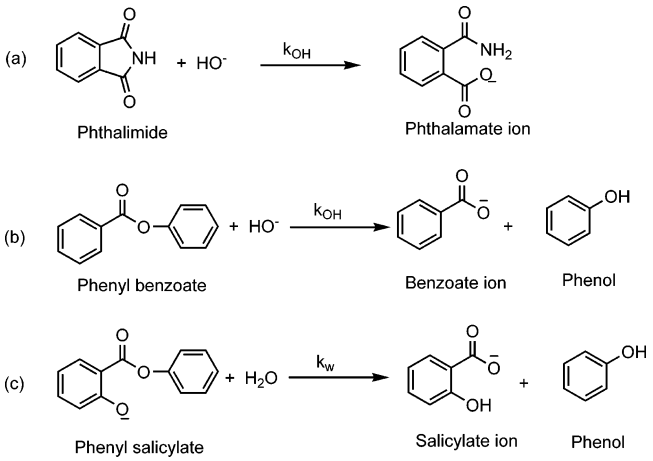

* Corresponding author. E-mail: niyaz@um.edu.my.

10.1021/jp073980j CCC: $37.00
Published on Web 10/03/2007

But such unusual observations were not obtained in the presence of $C_{16}E_{20}$ micelles under essentially similar conditions.[5,8] The observed data, obtained at $R < R_t$, fit satisfactorily to the PM model of the micelle. Perhaps the most unusual observation, revealed by recent studies,[5,6,9] is an apparent depletion of hydroxide ions and water molecules from $C_{12}E_{23}$ micellar environment where organic substrate molecules (sub = PSH, PB, phthalimide, and 4-nitrophthalimide) reside, and consequently, it causes irreversible trapping of sub molecules by micelles at R values $> R_t$. Such irreversible micellar trapping of sub molecules is expected to increase with the increase in hydrophobicity of sub molecules. The present study was initiated to explore the possibility of micellar irreversible portioning of reactants HO^- and *N*-benzylphthalimide (**1**), a nonionizable and more hydrophobic imide compared with phthalimide, in the $C_{16}E_{20}$ and $C_{16}E_{10}$ micellar-mediated alkaline hydrolysis of **1**.

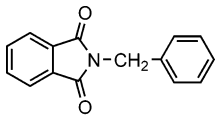

1

The observed data and their plausible explanations are described in this manuscript.

Experimental Section

Materials. Reagent-grade polyoxyethylene (20) cetyl ether $\{C_{16}H_{33}(OCH_2CH_2)_{20}OH$ (Brij 58 or $C_{16}E_{20})\}$ and polyoxyethylene (10) cetyl ether $\{C_{16}H_{33}(OCH_2CH_2)_{10}OH$ (Brij 56 or $C_{16}E_{10})\}$ were commercial products of highest available purity. All other chemicals were also of reagent-grade. *N*-Benzylphthalimide (**1**) and *N*-benzylphthalamic acid (**2**) were synthesized as described in an earlier reports.[10] Stock solutions (0.01 M) of **1** were prepared in acetonitrile.

Kinetic Measurements. The rate of hydrolysis of **1**, in an alkaline medium, was studied by monitoring the disappearance of reactant **1** spectrophotometrically at 300 nm. In a typical kinetic run, the reaction mixture (total volume of either 4.9 cm^3 for fast reactions with half-life of <1.6 h or 14.7 cm^3 for slow reaction with half-life of >5 h) containing all the reaction ingredients except **1** was equilibrated at 35 °C (using a thermostated water bath) for 5−10 min. The reaction was then started by adding 0.1 cm^3 (to 4.9 cm^3) or 0.3 cm^3 (to 14.7 cm^3) of reaction mixture of 0.01 M **1** (prepared in CH_3CN). The final total volume of the reaction mixture in each kinetic run was 5 cm^3 (for fast reaction) or 15 cm^3 (for slow reaction). An aliquot of ∼2.5 cm^3 was quickly transferred to a 3 cm^3 quartz cuvette kept in the thermostated cell compartment of the UV−vis double-beam spectrophotometer. The decrease in absorbance (A_{obs}) at 300 nm as a function of reaction time (t) for fast reaction was monitored by the spectrophotometer. A sampling technique was used to monitor the disappearance of **1** spectrophotometrically at 300 nm as a function of reaction time (t) for slow reactions.

All the kinetic runs were carried out under essentially pseudo-first-order kinetic conditions, and pseudo-first-order rate constants (k_{obs}) were calculated from eq 1

$$A_{obs} = \delta_{app}[R_0] \exp(-k_{obs}\, t) + A_\infty \qquad (1)$$

with nonlinear least-squares technique considering δ_{app} (apparent molar absorptivity of the reaction mixture) and A_∞ (the absorbance of the reaction mixture at reaction time $t = \infty$) also as unknown kinetic parameters.[11] In eq 1, A_{obs} represents absorbance of the reaction mixture at any reaction time t and $[R_0]$ is the initial concentration of **1**. The reactions were carried out for up to 7−9 half-lives, and the observed data (A_{obs} vs t) fitted well to eq 1 as is evident from low values of standard deviations associated with the calculated kinetic parameters, k_{obs}, δ_{app}, and A_∞ (Tables S1−S4, Supporting Information) as well as from the least-squares predicted solid lines of Figure 5. The molar absorptivities of ionized and nonionized *N*-benzylphthalamic and phthalic acids as well as benzylamine at 300 nm are very low (∼40 M^{-1} cm^{-1}). Therefore, $\delta_{app} \approx \delta_{\mathbf{1}}$ at 300 nm because $\delta_{app} = \delta_{\mathbf{1}} - \delta_P$, where $\delta_{\mathbf{1}}$ and δ_P represent the molar absorptivity of **1** and product (*N*-benzylphthalamic acid, **2**), respectively.

Most of the kinetic runs were carried out at low hydroxide ion concentration (7.6×10^{-4} to 2.0×10^{-3} M NaOH) simply because of the rather high value of the second-order rate constant (k_{OH} = 22 M^{-1} s^{-1} at 35 °C) for hydroxide ion-assisted hydrolysis of **1**.[10] However, we did not use any special device to protect reaction mixtures from atmospheric CO_2 except usual ones: using ≥5 M NaOH stock solution and freshly glass-distilled water. The stock solutions of lower hydroxide ion concentrations were prepared in freshly glass-distilled water. Reactions were carried out in properly stoppered reaction vessels and cuvettes. The average values of k_{OH} (obtained from ≥5 kinetic runs) at 7.6×10^{-4}, 1.0×10^{-3}, and 2.0×10^{-3} M NaOH as well as within the $[C_mE_n]_T$ (m = 16, n = 20, 10) range from 0.0 to <cmc are 17.8 ± 0.6 and 21.0 ± 0.4 M^{-1} s^{-1} for $C_{16}E_{10}$ as well as 20.9 ± 0.3 and 26.6 ± 0.1 M^{-1} s^{-1} for $C_{16}E_{20}$. These values of k_{OH} are not appreciably different from 22 M^{-1} s^{-1} derived from k_{obs} values obtained at 1.0 M ionic strength, 35 °C, and within the [NaOH] range of 3.0×10^{-3} to 5.0×10^{-3} M.[10] The observed data (A_{obs} vs t) revealed good fit to eq 1 for entire kinetic runs (Tables S1−S4, Supporting Information) within the reaction period of 7−9 half-lives. An appreciable problem caused by the atmospheric CO_2 could have resulted in bad data fit or even departure from data fit to eq 1 for kinetic runs carried out at higher values of $[C_mE_n]_T$. Thus, these observations rule out the presence of a kinetically detectable probable problem caused by atmospheric CO_2 under such alkaline reaction conditions.

It should be noted that the rate of alkaline hydrolysis of **2** is expected to be extremely slow. An attempt to study the rate of alkaline hydrolysis of **2** was unsuccessful because of the instability of the hydrolysis products (benzylamine and phthalic acid) in a highly alkaline aqueous solution containing 2% v/v *N*,*N*-dimethylformamide (DMF). However, the values of A_{obs} of an aqueous mixture containing 1.0×10^{-3} M benzylamine, 1.0×10^{-3} M phthalic acid, 1.0 M NaCl, and 4% v/v DMF remained unchanged at 35 °C, and 265 nm within a period of ∼16 h. But, the values of A_{obs} of the reaction mixture containing 1.0×10^{-3} M **2**, 0.5 M NaOH, 1.5 M NaCl, and 2% v/v DMF showed a decrease of 0.005 absorbance units within 16 h of the progress of the reaction. The decrease of 0.005 absorbance units constitutes 3.6% progress of the alkaline hydrolysis of **2** within 16 h, and thus, these results give $k_{obs} = 6 \times 10^{-7}$ s^{-1}. The value of the second-order rate constant (k_{OH}) for the reaction of HO^- with **2** is then equal to 1.2×10^{-6} M^{-1} s^{-1}. Although the value of k_{OH} ($= 1.2 \times 10^{-6}$ M^{-1} s^{-1}) is not very reliable because of extremely low values of absorbance change (0.005 absorbance units) in ∼16 h, it may be compared with the reported values of k_{OH} for the reaction of HO^- with *N*-methylbenzanilide,[12] benzamide,[13] *N*-methylbenzamide,[13] and *N*,*N*-dimethylbenzamide[13] as 2.2×10^{-6}, 6.1×10^{-7}, 2.3×10^{-7}, and 5.8×10^{-7} M^{-1} s^{-1}, respectively.

SCHEME 2

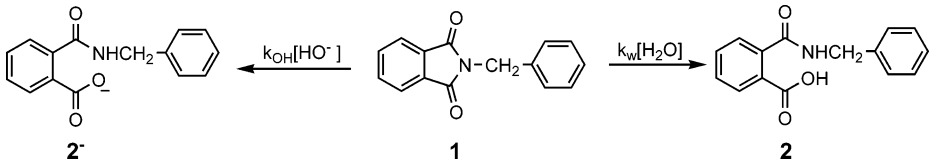

Product Characterization. The alkaline hydrolysis of **1** in an aqueous reaction mixture containing 2.0×10^{-4} M **1**, 2.0×10^{-3} M NaOH, 5.0×10^{-2} M $C_{16}E_{20}$, and 2% v/v CH_3CN was allowed to progress for the reaction period of more than 10 half-lives before the UV absorption spectrum of this reaction mixture was obtained. The UV absorption spectrum of the reaction mixture turned out to be similar to a typical UV absorption spectrum of an authentic sample of **2** obtained under identical experimental conditions. A similar spectral study also showed **2** as the alkaline hydrolysis product of **1** in the presence of $C_{16}E_{10}$ micelles.

One of the reviewers has pointed out that nonionic surfactants are notoriously prone to air oxidation. But such an effective air oxidation of $C_{16}E_{20}$ and $C_{16}E_{10}$ may be expected to (i) cause problem in the observed data fit to eq 1 and (ii) reveal a spectrum of product(s) not exactly similar to the spectrum of the expected hydrolysis product **2**. But the observed data (A_{obs} vs t) for the entire kinetic runs fit well to eq 1 for the reaction period of 7−9 half-lives, and the product spectra turned out to be exactly similar to the spectrum of an authentic sample of **2** under similar experimental conditions as mentioned in Kinetic Measurements and Product Characterization sections, respectively. Similar observations were obtained in earlier published work on the effects of nonionic surfactants and mixed nonionic−cationic surfactants on the rates of alkaline hydrolysis of PB, PSH, phthalimide, and 4-nitrophthalimide where the effects of $C_{12}E_{23}$ micelles on the reaction rates were similar to what was obtained with $C_{16}E_{10}$ in the present study. It seems highly unlikely that the effective air oxidation could have no effect on the observed data fit to kinetic equation(s) for first-order rate of alkaline hydrolysis as well as UV spectra of the products of all these reactions.

As mentioned earlier in the text, we did notice the problem of the fitting of the observed data to eq 1 for hydrolysis of authentic **2** under highly alkaline medium. This problem has been ascertained as due to the instability of the product mixture (benzylamine + phthalic acid) + 4% v/v DMF solvent under such highly alkaline medium.

Results and Discussion

The rate of alkaline hydrolysis of **1** in the absence of micelles obeys the following rate law

$$\text{rate} = (k_w + k_{OH}[HO^-])[\mathbf{1}] \qquad (2)$$

where k_w is the pseudo-first-order rate constant for pH-independent hydrolysis of **1** and k_{OH} is the second-order rate constant for the reaction of **1** with HO^-. Thus, a brief reaction scheme for alkaline hydrolysis of **1** may be represented by Scheme 2. The pseudo-first-order rate constant (k_w) for pH-independent hydrolysis of **1** (i.e., reaction between H_2O and **1**) may be expected to be $\sim 10^{-10}$ s^{-1} because the reported value of k_{obs} for hydrolysis of *N*-methylphthalimide is 3×10^{-10} s^{-1} at 0.03 M HCl, and 30 °C.[14] The value of k_w remained negligible compared with $k_{OH}[HO^-]$ at $[HO^-] \geq 3.0 \times 10^{-3}$ M, and the value of k_{OH} is 21.8 M^{-1} s^{-1} at 35 °C.[10]

SCHEME 3

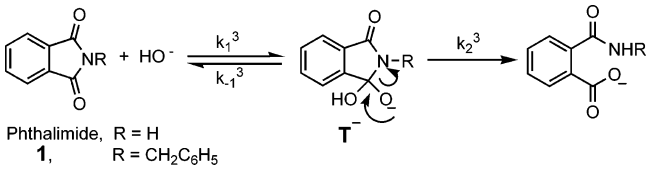

Effects of $[C_{16}E_{20}]_T$ on k_{obs} for Hydrolysis of 1 at 1.0×10^{-3} and 2.0×10^{-3} M NaOH and 35 °C. The rate of hydrolysis of **1** was studied within the total concentration of $C_{16}E_{20}$ ($[C_{16}E_{20}]_T$) ranging from 5.0×10^{-6} to 1.7×10^{-1} M at both 1.0×10^{-3} and 2.0×10^{-3} M NaOH. The values of k_{obs} showed an apparent monotonic decrease with the increase in $[C_{16}E_{20}]_T$ from 7.0×10^{-5} to 1.7×10^{-1} M at 1.0×10^{-3} M NaOH and from 2.0×10^{-5} to 1.7×10^{-1} M at 2.0×10^{-3} M NaOH. The values of k_{obs}, δ_{app}, and A_∞, obtained under such conditions, are summarized in Tables S1 and S2 (Supporting Information). Since the mechanism of a reaction remains generally unchanged with the change in the reaction medium from pure aqueous to aqueous micelles, the hydrolytic cleavage of **1** in the micellar pseudophase may also be expected to involve HO^- and **1** as the reactants. The reaction mechanism for hydroxide ion-assisted hydrolysis of phthalimide, N-alkyl-, and N-aryl-substituted phthalimides in aqueous solvent containing 2% v/v CH_3CN may be shown in Scheme 3 where the k_1^3 step is the rate-determining step.[15] In Scheme 3, T^- represents highly reactive monoanionic tetrahedral intermediate.

The values of δ_{app} at 1.0×10^{-3} M NaOH remained almost unchanged at $\sim < 4.0 \times 10^{-4}$ M $C_{16}E_{20}$ followed by a modest but gradual decrease until $[C_{16}E_{20}]_T \approx 1.2 \times 10^{-1}$ M. But a significant large decrease (∼45%) in δ_{app} is visible with the increase in $[C_{16}E_{20}]_T$ from$\sim 1.4 \times 10^{-1}$ to 1.7×10^{-1} M (Figure 1 and Table S1, Supporting Information). However, at 2.0×10^{-3} M NaOH, the decrease in δ_{app} is only ∼15% with the increase in $[C_{16}E_{20}]_T$ from 5.0×10^{-4} to 1.7×10^{-1} M (Figure 1 and Table S2, Supporting Information). Such characteristic observations were not observed in the alkaline hydrolysis of phthalimide at 0.02 M NaOH, 35 °C, and within the $[C_{16}E_{20}]_T$ range of 1.0×10^{-4} to 1.8×10^{-1} M[5] which could be attributed to (i) the 20-fold larger value of NaOH and (ii) the expected nonionic micellar deeper penetration of **1** compared to that of phthalimide because of the higher hydrophobicity of **1** compared to that of phthalimide.

The nonlinear decrease in k_{obs} with increase in $[C_mE_n]_T$ ($m = 16$, $n = 20$, 10) may be explained using the PM model[16] which consists of several assumptions.[17] The reaction scheme for the hydrolysis of **1**, in the presence of C_mE_n micelles (D_n), is shown in Scheme 4 where subscripts W and M represent aqueous (or water) phase and micellar pseudophase, respectively. The experimentally observed rate law (rate $= k_{obs}[\mathbf{1}]_T$ where $[\mathbf{1}]_T = [\mathbf{1}_W] + [\mathbf{1}_M]$) and Scheme 4 can lead to eq 3

$$k_{obs} = \frac{k_W + k_M K_S[D_n]}{1 + K_S[D_n]} \qquad (3)$$

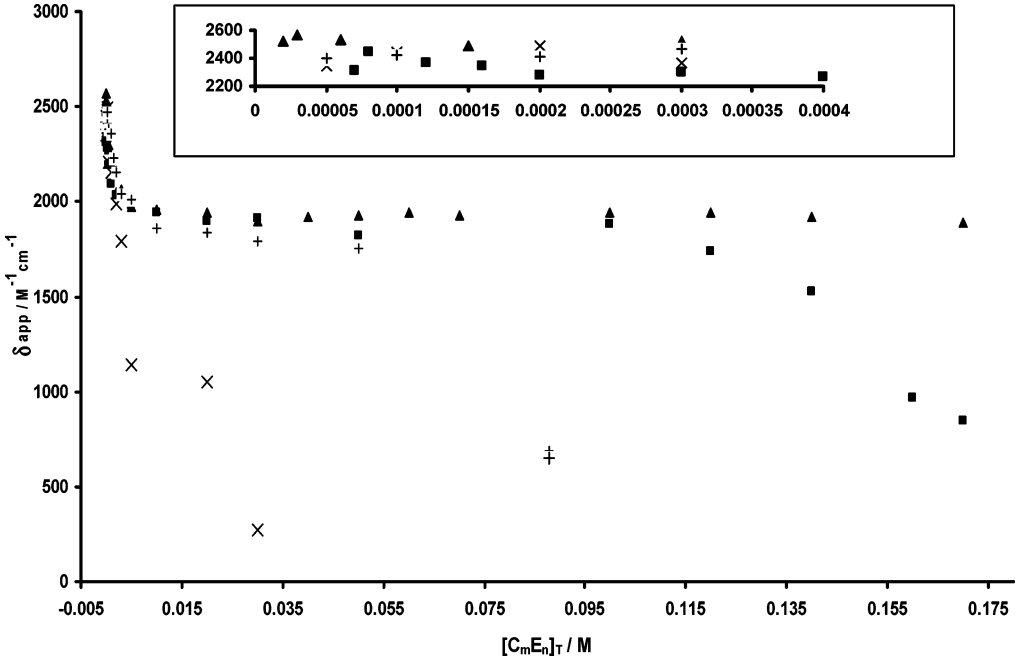

Figure 1. Graphical representation of δ_{app} vs $[C_mE_n]_T$ for hydrolysis of **1** at 1.0×10^{-3} (■) and 2.0×10^{-3} M (▲) NaOH in the presence of $C_{16}E_{20}$ micelles as well as at 7.6×10^{-4} (×) and 1.0×10^{-3} M (+) NaOH in the presence of $C_{16}E_{10}$ micelles.

SCHEME 4

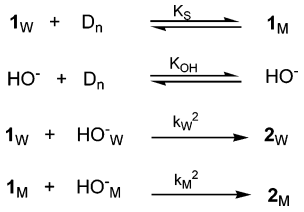

where $k_W = k_W^2[HO^-]_T$ with $[HO^-]_T = [HO^-_M] + [HO^-_W]$, $k_M = (k_M^2 K_{OH}[HO^-]_T)/V_M$ with V_M representing molar volume of the micellar reaction region,[1,17a,b,d,18] $1 \gg K_{OH}[D_n]$ as well as K_s and K_{OH} are the respective micellar binding constants of **1** and HO^-. In eq 3, $[D_n] = [C_mE_n]_T -$ cmc with cmc representing the critical micelle concentration.

The values of k_M ($= k_M^{mr} K_{OH}[HO^-]_T$ with $k_M^{mr} = k_M^2/V_M$) and K_S were calculated from eq 3 considering k_W and cmc as known parameters. The value of k_W was obtained experimentally by carrying out kinetic run at $[C_{16}E_{20}]_T = 0$, and the value of cmc was determined by graphical technique[19] as well as by an iterative technique.[20] The nonlinear least-squares calculated respective values of k_M and K_S are shown in Table 1. The values of cmc, obtained from respective graphical and iterative techniques, are 2.88×10^{-5} and 2.91×10^{-5} M at 1.0×10^{-3} M NaOH as well as 8.75×10^{-6} and 1.70×10^{-6} M at 2.0×10^{-3} M NaOH. However, it is worth mentioning that an increase in cmc from 0.0 to 1.0×10^{-5} M did not change appreciably the values of k_M and K_S (Table 1) while the value of $\sum d_i^2$ changed from 5.30×10^{-6} to 6.00×10^{-6}. ($d_i = k_{obs,i} - k_{calcd,i}$ with $k_{obs,i}$ and $k_{calcd,i}$ representing the respective observed and calculated values of rate constants at the ith value of $[C_{16}E_{20}]_T$.) These calculated values of least-squares ($\sum d_i^2$) and kinetic parameters (k_M and K_S) show that an increase in cmc from 0.0 to 1.0×10^{-5} M did not change them significantly, and hence, an appreciable error in cmc is not a setback for data analysis. The reported values of cmc for $C_{16}E_{12}$, $C_{12}E_{10}$, and $C_{12}E_{23}$ are 2×10^{-6}, 100×10^{-6}, and 140×10^{-6} M, respectively, obtained in the absence of any ionic or nonionic solute.[21]

TABLE 1: Values of k_M and K_S Calculated from Eq 3 for Alkaline Hydrolysis of 1 at Different [NaOH]

C_mE_n	10^4 [NaOH] M	10^6 cmc M	$10^4\ k_W$ s^{-1} [a]	$10^4\ k_M$ s^{-1}	$10^{-2}\ K_S$ M^{-1}
$C_{16}E_{20}$	10.0	28.8	209 ± 3[b]	1.56 ± 1.28[b]	10.4 ± 0.4[b]
	20.0	0.0	532 ± 2	6.28 ± 1.60	10.6 ± 0.2
		8.75	532 ± 2	6.74 ± 1.67	10.8 ± 0.2
		10.0	532 ± 2	6.80 ± 1.70	10.9 ± 0.2
$C_{16}E_{10}$	7.6	31.3	135 ± 5	-39 ± 8	6.0 ± 0.7
		31.3	135 ± 5	0	12.5 ± 8.4
	10.0	33.0	210 ± 4	-1.7 ± 3.5	6.6 ± 0.4
		33.0	210 ± 4	0	6.7 ± 0.9

[a] The values of k_W were obtained from k_{obs} values obtained within $[C_mE_n]_T$ ($m = 16$ and $n = 10$, 20) range from 0.0 to <cmc. [b] Error limits are standard deviations.

The calculated values of k_M are associated with ~80% and ~25%, while the values of K_S are associated with ~4% and 2% standard deviations at 1.0×10^{-3} and 2.0×10^{-3} M NaOH, respectively (Table 1). Considerably high standard deviation (~80%) with k_M at 1.0×10^{-3} M NaOH merely reveals that the value of k_M is not reliable. The observed kinetic data (k_{obs} vs $[C_mE_n]_T$) fit to eq 3 satisfactorily in terms residual errors ($= k_{abs,i} - k_{calcd,i}$ where subscript i represents data at ith values of $[C_mE_n]_T$) until fractions of micellized **1** become 95% and 98% at 1.0×10^{-3} and 2.0×10^{-3} M NaOH, respectively. The micellar shape, size, and packing parameters generally change with the increase in the micelle-forming surfactant concentrations, and consequently, the observed kinetic data may not be expected to fit to eq 3 within a large range of surfactant concentrations. The standard deviation associated with the K_S value is only 4% at 1.0×10^{-3} M NaOH. Thus, ~80% and 4% standard deviations associated with the respective k_M and K_S at 1.0×10^{-3} M NaOH may be attributed to the insignificant contribution of $k_M K_S[D_n]$ compared to k_W in the numerator of eq 3 within the $[C_{16}E_{20}]_T$ range where residual errors are low. The kinetic data in Table S1 (Supporting Information) reveal ~19%, 13%, and 7% contributions of $k_M K_S[D_n]$ compared to k_W at 0.03, 0.02, and 0.01 M $C_{16}E_{20}$, respectively.

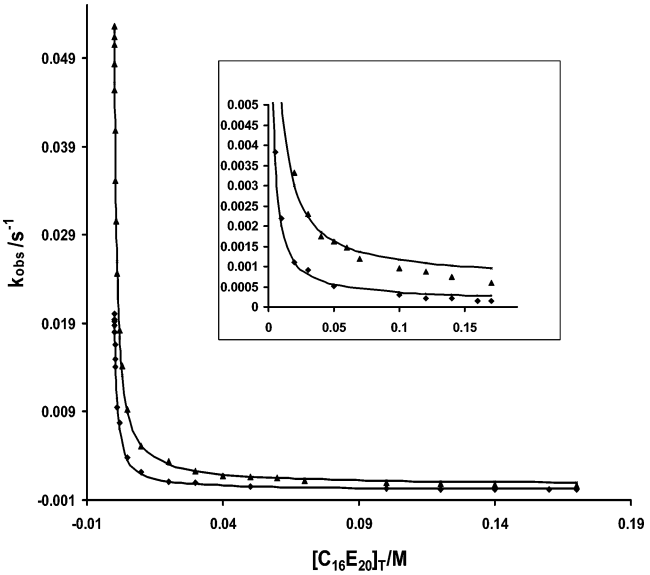

Figure 2. Plots showing the dependence of k_{obs} upon $[C_{16}E_{20}]_T$ for hydrolysis of **1** at 1.0×10^{-3} (◆) and 2.0×10^{-3} M (▲) NaOH. The solid lines are drawn through the calculated rate constants (k_{calcd}) obtained from eq 3 with 10^5cmc = 2.88 M, 10^3 k_W = 20.9 s^{-1}, 10^4 k_M = 1.56 s^{-1}, and 10^{-3} K_S = 1.04 M^{-1} for (◆) and 10^6 cmc = 8.75 M, 10^3 k_W = 53.2 s^{-1}, 10^4 k_M = 6.74 s^{-1}, and 10^{-3} K_S = 1.08 M^{-1} for (▲).

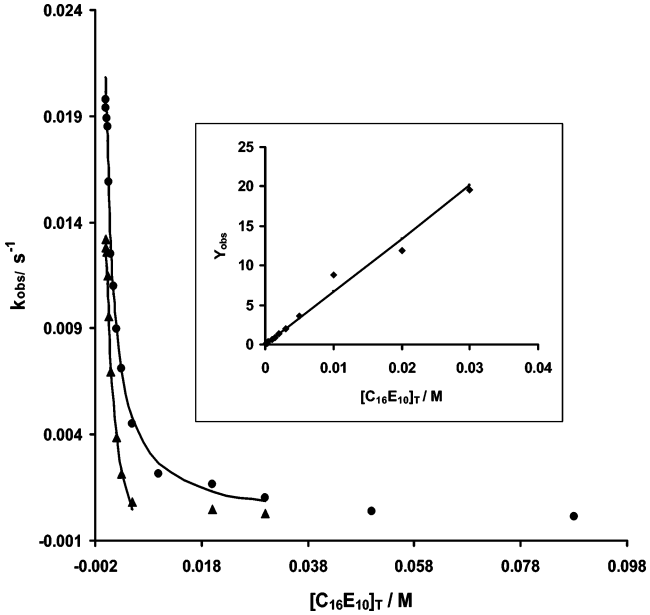

Figure 3. Plots of k_{obs} vs $[C_{16}E_{10}]_T$ for hydrolysis of **1** at 7.6×10^{-4} (▲) and 1.0×10^{-3} (●) M NaOH in the presence of $C_{16}E_{10}$ micelles. The solid lines are drawn through the calculated rate constants (k_{calcd}) obtained from eq 3 with 10^5 cmc = 3.13 M, 10^3 k_W = 13.5 s^{-1}, 10^3 k_M = −3.9 s^{-1}, and 10^{-2} K_S = 6.0 M^{-1} for (▲) and 10^5cmc = 3.30 M, 10^3 k_W = 21.0 s^{-1}, 10^4 k_M = −1.7 s^{-1}, and 10^{-2} K_S = 6.6 M^{-1} for (●). Inset: Plot showing the dependence of Y_{obs} upon $[C_{16}E_{10}]_T$ for hydrolysis of **1** at 1.0×10^{-3} M NaOH (◆) where $Y_{obs} = (k_W - k_{obs})/k_{obs}$ with 10^3 k_W = 21.0 s^{-1} and the solid line is drawn through the Y_{calcd} values which were obtained from the relationship $Y_{obs} = K_S[D_n]$ with 10^{-2} K_S = 6.72 M^{-1} and $[D_n] = [C_{16}E_{10}]_T$ − cmc with 10^5cmc = 3.30 M.

An apparent satisfactory fit of observed data to eq 3 is evident from the plots of Figure 2 where the solid lines are drawn through the least-squares calculated rate constant (k_{calcd}) values. However, increasing negative deviations (∼16−87%) of k_{obs} values compared to the corresponding k_{calcd} values could be seen at 1.0×10^{-3} M NaOH and ≥0.10 M $C_{16}E_{20}$ (Figure 2 and Table S1, Supporting Information). Similarly, k_{obs} values show ∼13−60% negative deviations compared to k_{calcd} values at 2.0×10^{-3} M NaOH and ≥0.10 M $C_{16}E_{20}$ (Figure 2 and Table S2, Supporting Information). Such observations were not obtained in $C_{16}E_{20}$ micellar-mediated hydrolysis of phthalimide at 2.0×10^{-2} M NaOH where the values of k_M and K_S turned out to be ∼0 and 7.5 M^{-1}, respectively.[5] This characteristic different effects of $[C_{16}E_{20}]_T$ on the rate of alkaline hydrolysis of **1** and phthalimide may be ascribed to (i) larger hydrophobicity of **1** than that of phthalimide, (ii) absence and presence of an acidic group of pK_a of 9−10 in, respectively, **1** and phthalimide, and (iii) considerably larger values of $[C_{16}E_{20}]_T/[NaOH]$ in the alkaline hydrolysis of **1** than that of phthalimide. Modest yet definite increasing negative deviations of k_{obs} values compared to the corresponding k_{calcd} values at ≥0.10 M $C_{16}E_{20}$ demonstrate that the values of k_M and K_S are no longer $[C_{16}E_{20}]_T$-independent at $[C_{16}E_{20}]_T \geq 0.10$ M. An alternative possibility that the inequality $1 \gg K_{OH}[D_n]$ is no longer true at $[C_{16}E_{20}]_T \geq 0.10$ M may be ruled out for the reason that negative deviations were not observed in alkaline hydrolysis of phthalimide under such conditions.[5] Furthermore, the absence of the inequality $1 \gg K_{OH}[D_n]$ requires that the K_{OH} value should be ≥2 M^{-1} which is certainly too high because K_S of the phthalimide anion is only 7.5 M^{-1} (phthalimide anion has larger hydrophobicity and delocalized charge compared to hydroxide ion).

Effects of $[C_{16}E_{10}]_T$ on k_{obs} for Hydrolysis of 1 at 7.6×10^{-4} and 1.0×10^{-3} M NaOH and 35 °C. A series of kinetic runs has been carried out at different $[C_{16}E_{10}]_T$ ranging from 5.0×10^{-5} to 8.8×10^{-2} M at 7.6×10^{-4} and 1.0×10^{-3} M NaOH, respectively. The values of k_{obs}, δ_{app}, and A_∞, calculated from eq 1 under such conditions, are summarized in Tables S3 and S4 (Supporting Information), at 7.6×10^{-4} and 1.0×10^{-3} M NaOH, respectively. The values of absorbance (A_{obs}) at 0.05 and 0.088 M $C_{16}E_{10}$ remained unchanged at respective A_{obs} values of 0.446 and 0.506 within the reaction period of ∼46 h at 7.6×10^{-4} M NaOH indicating almost complete irreversible micellar partitioning of two reactants, **1** and HO^-, under such conditions. Similar observations were obtained in the $C_{12}E_{23}$ micellar-mediated alkaline hydrolysis of phthalimide under the typical reaction conditions.[5]

Perhaps it is noteworthy that the reaction mixture containing 2.0×10^{-4} M **1**, 1.0×10^{-3} M NaOH, and 1.0×10^{-2} M $C_{16}E_{10}$ became highly viscous at ambient temperature (∼27 °C). The increase in $[C_{16}E_{10}]_T$ beyond 1.0×10^{-2} M caused precipitation into the reaction mixtures at ambient temperature. But the same reaction mixtures became clear solutions at 35 °C. Such observations were not obtained at 1.0×10^{-2} M $C_{16}E_{20}$ under similar conditions. It is well-known that the increase in the concentration of micelle-forming surfactant generally changes the structure of the micelle from spherical to cylindrical, rodlike, or disklike.[2] But such ionic micellar structural transitions are generally insensitive to the rate of reaction. However, such nonionic micellar structural transition, under extreme conditions such as considerably high concentration of surfactant, might affect the rate of reaction due to breakdown of some basic assumption(s) of the PM model.

The observed data (k_{obs} vs $[C_{16}E_{10}]_T$), obtained within $[C_{16}E_{10}]_T$ range of 5.0×10^{-5} to 8.8×10^{-2} M at 1.0×10^{-3} M NaOH and 5.0×10^{-5} to 5.0×10^{-3} M at 7.6×10^{-4} M NaOH, were treated with eq 3, and nonlinear least-squares calculated respective values of k_M and K_S are summarized in Table 1. The values of k_{calcd}, as shown in Tables S3 and S4 (Supporting Information) and Figure 3, show that the fitting of observed data to eq 3 is good within the $[C_{16}E_{10}]_T$ range of 5.0×10^{-5} to 5.0×10^{-3} M at 7.6×10^{-4} M NaOH and $5.0 \times$

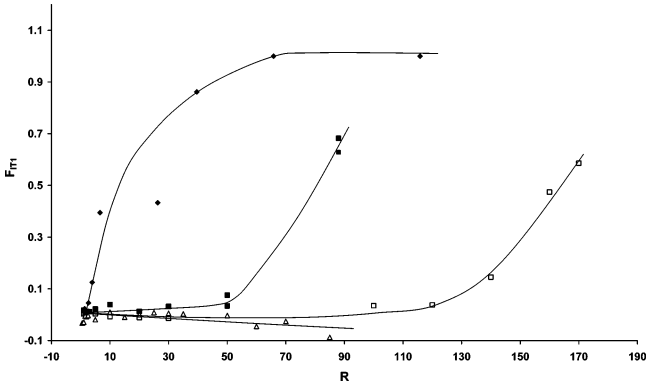

Figure 4. Plots showing the dependence of F_{IT1} vs R (where $R = [C_mE_n]_T/[NaOH]$ with $m = 16$ and $n = 20$, 10) for $C_{16}E_{20}$, (△) at 2.0×10^{-3} M NaOH, (□) at 1.0×10^{-3} M NaOH and for $C_{16}E_{10}$, (■) at 1.0×10^{-3} M NaOH, (◆) at 7.6×10^{-4} M NaOH.

10^{-5} to 3.0×10^{-2} M at 1.0×10^{-3} M NaOH. However, the calculated negative values of k_M are physically/chemically meaningless, and consequently the values of K_S were also calculated from eq 3 with $k_M = 0$, and such calculated K_S values are also shown in Table 1. The calculated value of K_S ($= 1.25 \times 10^3$ M^{-1}) at 7.6×10^{-4} M NaOH is not reliable because it is associated with high standard deviation (~70%) which is due to poor fitting of observed data to a linearized form of eq 3 with $k_M = 0$.

The value of the ratio of K_S of **1** with $C_{16}E_{20}$ ($K_S = 1.04 \times 10^3$ M^{-1}) and $C_{16}E_{10}$ ($K_S = 670$ M^{-1}) may be compared with the corresponding ratio of K_S of benzonitrile oxide with $C_{16}E_{20}$ ($K_S = 38$ M^{-1}) and $C_{16}E_{10}$ ($K_S = 27$ M^{-1}).[22] The nearly 90-fold smaller value of k_M than that of k_W for $C_{16}E_{10}$ micelles cannot be explained in terms of a micellar medium effect only because such an effect should not decrease k_M by more than ~5-fold compared with k_W because pseudo-first-order rate constants for alkaline hydrolysis of **1** at 2.0×10^{-3} M NaOH decreased by ~5-fold with the increase in acetonitrile content from 2% to 80% v/v in mixed aqueous solvent at 35 °C. Generally the reaction mechanism of an addition elimination reaction does not change with the change in solvent from pure aqueous to mixed aqueous−organic solvent, and the aqueous reaction mechanism for alkaline hydrolysis of **1** is shown in Scheme 3. Perhaps an equal or even more effective cause for the insignificant rate of alkaline hydrolysis of **1** in the micellar pseudophase compared with that in the aqueous phase may be attributed to the extremely low concentration of hydroxide ions in the vicinity of the micellized **1** molecules due to different average locations of HO^- ions and **1** molecules in the micellar pseudophase. Similarly, the values of k_M turned out to be ~0 for alkaline hydrolysis of phthalimide in $C_{16}E_{20}$ micelles[5] and securinine in $C_{12}E_{10}$ micelles[23] while K_S values for anionic phthalimide with $C_{16}E_{20}$ micelles and securinine with $C_{12}E_{10}$ micelles are 7.5 and 14.8 M^{-1}, respectively.

Evidence for an Irreversible $C_{16}E_{10}$ and $C_{16}E_{20}$ Micellar Binding of 1 Under the Typical Reaction Conditions. As mentioned earlier in the Experimental Section, $\delta_{app} = \delta_1 - \delta_2$ where $\delta_1 \approx 2400$ M^{-1} cm^{-1} and $\delta_2 \approx 40$ M^{-1} cm^{-1} at 300 nm. The values of δ_{app} should be independent of $[C_mE_n]_T$ if the values of δ_1 and δ_2 are independent of $[C_mE_n]_T$. However, a decrease in δ_{app} with increase in $[C_mE_n]_T$ (Figure 1) may be attributed to (i) decrease in δ_1 with increase in $[C_mE_n]_T$ while δ_2 is independent of $[C_mE_n]_T$, (ii) increase in δ_2 with the increase in $[C_mE_n]_T$ while δ_1 is independent of $[C_mE_n]_T$, (iii) decrease in δ_1 and increase in δ_2 with the increase in $[C_mE_n]_T$, and (iv) irreversible micellar trapping of nonreacted **1** while the values of δ_1 and δ_2 are independent of increasing $[C_mE_n]_T$. But the values of A_T and A_{T+2} in Tables S1−S4 (Supporting Information), show that the values of δ_2 are independent of $[C_mE_n]_T$ while ~20% decrease in δ_{app} with increased in $[C_{16}E_{20}]_T$ from 2.0×10^{-5} to 0.17 M at 2.0×10^{-3} M NaOH shows a mild decrease in δ_1 values under such conditions (Figure 1). Thus, the significant decrease in δ_{app} at certain typical values of $[C_mE_n]_T$ and [NaOH] is due to primarily reason iv. The value of A_0 ($A_0 = A_{obs}$ at $t = 0$) at a constant $[C_mE_n]_T$ is the sum of absorbance (A_1) contributed by [**1**] and A_T contributed by microturbidity if any. Thus, $A_0 = A_1 + A_T$. Similarly, the value of A_∞ ($A_\infty = A_{obs}$ at $t = \infty$) at a constant $[C_mE_n]_T$ is the sum of A_2 (due to [**2**]), A_T (due to microturbidity if any), and A_{IT1} (due to irreversibly micelle-trapped **1**). Thus, the fraction of irreversibly micelle-trapped **1** at $t = \infty$ ($F_{IT1} = A_{IT1}/A_1$) may be given as

$$F_{IT1} = (A_\infty - A_{T+2})/(A_0 - A_T) \quad (4)$$

where A_{T+2} represents the sum of the absorbance values due to microturbidity A_T (if any) and A_2. The values of A_T and A_{T+2} at different $[C_{16}E_{20}]_T$ and $[C_{16}E_{10}]_T$ were determined at 300 nm under the reaction conditions of kinetic runs at the respective [**1**] = [**2**] = 0 and [**1**] = 0 while [**2**] = 2.0×10^{-4} M. These results are summarized in Tables S1−S4 (Supporting Information). The values of F_{IT1} were calculated from eq 4 at a constant [NaOH] and different $[C_{16}E_{20}]_T$ or $[C_{16}E_{10}]_T$, and these values are shown as plots of F_{IT1} versus $[C_mE_n]/[NaOH]$ (with $m = 16$ and $n = 20$, 10) in Figure 4.

Figure 4 reveals the presence of significant amounts of micelle-trapped nonreacted **1** at ≥0.14 M $C_{16}E_{20}$ and 1.0×10^{-3} M NaOH, ≥0.088 M $C_{16}E_{10}$ and 1.0×10^{-3} M NaOH, and ≥3.0×10^{-3} M $C_{16}E_{10}$ and 7.6×10^{-4} M NaOH. If such micellar trapping of nonreacted **1** is indeed an irreversible process, then the values of A_{obs} at $t \geq 10$ half-lives (t at ~10 half-lives of a reaction is equivalent to t_∞ because more than 99.9% of the reaction is completed at $t = 10$ half-lives and, thus, A_{obs} at $t = 10$ half-lives may be considered as A_∞) should remain unchanged with increase in reaction time t at $t \approx 10$ half-lives or at t where $A_{obs} \approx A_\infty$. In order to test this conclusion, the reaction mixtures at $t \approx 10$ half-lives, under a variety of reaction conditions where Figure 4 predicts the presence of nonreacted **1**, were left at 35 °C for a reaction period of ≤400 h, i.e., $\leq 10^3$ half-lives. These results, as summarized in Table 2, show that A_{obs} at $t \approx 10$ half-lives or at $t = \infty$ remained essentially unchanged with further increase in t, from $t \approx 10$ half-lives to $t \leq 10^3$ half-lives, which supports the conclusion of near-irreversible micellar trapping of nonreacted **1**.

It is evident from Figure 4 and Table 2 that the fraction of **1** trapped by nonionic micelles increases with increases in R ($= [C_{16}E_{10}]_T/[NaOH]$ or $[C_{16}E_{20}]_T/[NaOH]$) at a typical value of R ($= R_t$). This shows that if inequality $R > R_t$ is changed to $R < R_t$ by external addition of a known amount of NaOH to the reaction mixture at $t \geq t_\infty$, then irreversible micelle-bound **1** would become reversible micelle-bound, and consequently, the rate of disappearance of **1** would follow eq 1 and the value of k_{obs} may then be compared with k_{obs} obtained by carrying out another kinetic run by the use of an authentic sample of **1** under essentially similar experimental conditions. Such an effort is described below.

Although Figure 4 revealed that $F_{IT1} \approx 0$ at 0.05 M $C_{16}E_{10}$ and 1.0×10^{-3} M NaOH, an attempt was made to affirm its validity. To 5.0 cm^3 of the reaction mixture containing 2×10^{-4} M **1**, 1.0×10^{-3} M NaOH, 0.05 M $C_{16}E_{10}$ (where $[C_{16}E_{10}]_T/[NaOH] = 50$) was added 0.05 cm^3 of 0.1 M NaOH

TABLE 2: Values of Observed Absorbance (A_{obs}) at Different Reaction Times (t) at $t \geq t_\infty$ for the Kinetic Runs with Significant Values of F_{IT1}[a]

10^4[NaOH]/M = 10					7.6				
$[C_{16}E_{20}]_T$ M	t h	A_{obs}	A_{calcd}[b]	$t_{1/2}$ h	$[C_{16}E_{10}]_T$ M	t h	A_{obs}	A_{calcd}[c]	$t_{1/2}$ h
0.12	16.3	0.304	0.313	17.3	0.005	2.0	0.163	0.164	8.0
	24.3	0.297	0.313	25.8		21.1	0.147	0.163	83.0
0.14	23.5	0.389	0.397	24.8		116	0.122		478
	65.4	0.391		68.9		216	0.133		891
0.16	23.6	0.536	0.545	18.4		381	0.176		1569
	79.1	0.530		61.6	0.020	2.0	0.200	0.205	5.0
	104	0.531		81.4		22.9	0.201		57.5
0.17	24.6	0.595	0.603	19.1		143	0.195		359
	66.4	0.594		51.8		244	0.208		612
	163	0.596		127		408	0.218		1025
					0.030	47.9	0.370	0.365	75.0
						143	0.357	0.365	223
						244	0.360		380
						408	0.373		636
					0.050	0.029	0.453		
						20.8	0.447		
						45.6	0.446		
						141	0.445		
					0.088	0.056	0.497		
						20.8	0.502		
						45.7	0.504		
						141	0.519		

[a] $[\mathbf{1}_0] = 2.0 \times 10^{-4}$ M, $T = 35$ °C, $\lambda = 300$ nm, reaction mixture for each kinetic run contained 2% v/v CH_3CN. [b] Calculated from eq 1 with kinetic parameters, k_{obs}, δ_{app}, and A_∞ listed in Table S1 (Supporting Information). [c] Calculated from eq 1 with kinetic parameters, k_{obs}, δ_{app}, and A_∞ listed in Table S3 (Supporting Information).

TABLE 3: Values of k_{obs}, δ_{app}, and A_∞, Calculated from Eq 1 for Alkaline Hydrolysis of 1 in the Presence of $C_{16}E_{10}$ Micelles[a]

$[C_{16}E_{10}]_T$ M	10^3 [NaOH] M	$10^4\ k_{obs}$ s^{-1}	$10^{-2}\ \delta_{app}$ $M^{-1}\ cm^{-1}$	$10^3\ A_\infty$	k_{OH} $M^{-1}\ s^{-1}$ [b]	F_{IT1}[c]
0.087[d]	10.9	85.5 ± 0.7[e]	11.0 ± 0.04[e]	110 ± 0.5[e]	0.78	0.47
0.086[f]	20.6	162 ± 2	11.3 ± 0.08	108 ± 0.6	0.79	0.48
0.085[g]	39.5	351 ± 11	14.0 ± 0.4	108 ± 1.0	0.89	0.60
0.087[h]	5.0	40.8 ± 1.3	19.2 ± 0.2	124 ± 4	0.82	
0.087	10.0	102 ± 3	21.7 ± 0.3	124 ± 3	1.02	
0.087	15.0	179 ± 5	25.8 ± 0.4	127 ± 3	1.19	
0.087	20.0	211 ± 3	24.8 ± 0.2	124 ± 1	1.06	
0.087	25.0	246 ± 4	24.5 ± 0.2	125 ± 2	0.98	
0.087	30.0	276 ± 9	24.5 ± 0.5	131 ± 4	0.92	
0.087	40.0	312 ± 16	23.3 ± 0.7	141 ± 5	0.78	
0.084	5.0	40.2 ± 1.0	19.4 ± 0.2	122 ± 3	0.80	
0.084	10.0	107 ± 4	22.0 ± 0.3	127 ± 4	1.07	
0.084	15.0	165 ± 4	24.9 ± 0.3	128 ± 3	1.10	
0.084	20.0	213 ± 5	25.1 ± 0.3	130 ± 3	1.06	
0.084	25.0	244 ± 8	24.2 ± 0.4	116 ± 4	0.98	
0.084	30.0	292 ± 6	26.7 ± 0.3	135 ± 2	0.97	
0.084	40.0	320 ± 14	23.0 ± 0.6	138 ± 4	0.80	

[a] $[\mathbf{1}_0] = 2.0 \times 10^{-4}$ M, 35 °C, $\lambda = 300$ nm, unless otherwise noted, aqueous reaction mixture for each kinetic run contained 2% v/v CH_3CN. [b] $k_{OH} = k_{obs}/[NaOH]$. [c] $F_{IT1} = \delta_{app}/\delta_{app}^0$ with $\delta_{app}^0 = 23.5 \times 10^2\ M^{-1}\ cm^{-1}$. [d] To 5.0 cm^3 of the reaction mixture (containing 2.0×10^{-4} M **1**, 0.088 M $C_{16}E_{10}$, and 1.0×10^{-3} M NaOH, Table S4, Supporting Information) was added 0.05 cm^3 of 1.0 M NaOH at reaction time (t) ≈72.4 h. Under such conditions, $\delta_{app} = F_{IT1}\delta_{app}^0$ where F_{IT1} represents the fraction of **1** irreversibly trapped by micelles and $\delta_{app}^0 = \delta_1 - \delta_2$. [e] Error limits are standard deviations. [f] To 5.0 cm^3 of reaction mixture (containing 2.0×10^{-4} M **1**, 0.088 M $C_{16}E_{10}$, and 1.0×10^{-3} M NaOH, Table S4, Supporting Information) was added 0.10 cm^3 of 1.0 M NaOH at reaction time (t) ≈73.1 h, $\delta_{app} = F_{IT1}\delta_{app}^0$. [g] To 5.0 cm^3 of reaction mixture (containing 2.0×10^{-4} M **1**, 0.088 M $C_{16}E_{10}$, and 1.0×10^{-3} M NaOH, Table S4, Supporting Information) was added 0.20 cm^3 of 1.0 M NaOH at reaction time (t) ≈74.1 h, and $\delta_{app} = F_{IT1}\delta_{app}^0$. [h] Reaction mixtures for all kinetic runs were freshly prepared, and $\delta_{app} = \delta_{app}^0$ under such conditions.

at $t = 23.5$ h. The values of A_{obs} of the resulting reaction mixture (= 0.063) (where $[C_{16}E_{10}]_T/[NaOH] \approx 25$) remained unchanged at 300 nm for ~0.5 h. A similar observation was obtained when 0.2 cm^3 of 0.1 M NaOH was added to 5.0 cm^3 of reaction mixture containing 2×10^{-4} M **1**, 1.0×10^{-3} M NaOH, and 0.05 M $C_{16}E_{20}$ at $t = 25.8$ h where $[C_{16}E_{10}]_T/[NaOH] = 1.3$. These observations reveal the absence of nonreacted **1** into the reaction mixture containing 1.0×10^{-3} M NaOH and 0.05 M $C_{16}E_{20}$ at $t = 23.5$ and 25.8 h. Thus, the value of $A_\infty = 0.074$ obtained for this kinetic run is only due to microturbidity and product **2** (2×10^{-4} M) (Table S4, Supporting Information).

Similarly, to 5.0 cm^3 of the reaction mixture containing 0.088 M $C_{16}E_{10}$, 1.0×10^{-3} M NaOH, and 2.0×10^{-4} M **1** (where $[C_{16}E_{10}]_T/[NaOH] = 88$) was added 0.05 cm^3 of 1.0 M NaOH at $t = 72.4$ h, and the absorbance change of the reaction mixture (where $[C_{16}E_{10}]_T/[NaOH] = 8.0$) was quickly monitored spectrophotometrically as a function of time (t) at 300 nm. The values of A_{obs}, which dropped from 0.281 at $t = 30$ s to 0.111 at $t = 1800$ s, were found to fit to eq 1 with least-squares calculated values of k_{obs}, δ_{app}, and A_∞ as summarized in Table 3. Similar kinetic runs were carried out at 20.6×10^{-3} and 39.5×10^{-3} M NaOH using 5.0 cm^3 of the reaction mixture,

SCHEME 5

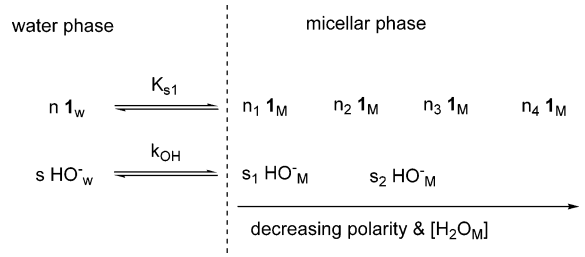

containing 0.088 M $C_{16}E_{10}$, 1.0×10^{-3} M NaOH, and 2.0×10^{-4} M **1**, withdrawn at, respectively, $t = 73.1$ and 74.1 h. The observed data (A_{obs} vs t) strictly followed eq 1, and the least-squares calculated kinetic parameters, k_{obs}, δ_{app}, and A_∞, from eq 1 are also summarized in Table 3. A few kinetics runs were also carried out on alkaline hydrolysis of authentic **1** at 35 °C, 2.0×10^{-4} M **1**, 0.084 and 0.087 M $C_{16}E_{10}$, and different values of [NaOH] ranging from 5.0×10^{-3} to 40.0×10^{-3} M. The spectrophotometrically observed data for these kinetic runs also strictly followed eq 1, and the least-squares calculated values of k_{obs}, δ_{app}, and A_∞ are also summarized in Table 3. The values of k_{OH} ($= k_{obs}$/[NaOH]) are nearly more than 20-fold smaller than k_{OH} value (21.8 M^{-1} s^{-1})[10] obtained under similar kinetic conditions in the absence of micelles, which could be ascribed to a merely micellar inhibitory effect (the fraction of micelle-bound **1** under such conditions is ≥ 0.98 where $K_S = 670$ M^{-1}).

It is evident from Table 3 that the values of k_{obs} obtained from the monotonic decreases in A_{obs} with t at 300 nm and 35 °C for the reaction mixture containing 2×10^{-4} M **1** and 0.088 M $C_{16}E_{10}$ when the value of [NaOH] was increased from 1.0×10^{-3} to 10.9×10^{-3} M at $t = 72.4$ h, from 1.0×10^{-3} to 20.6×10^{-3} M at $t = 73.1$ h, and from 1.0×10^{-3} to 39.5×10^{-3} M at $t = 74.1$ h are not significantly different from the corresponding k_{obs} values obtained for alkaline hydrolysis of authentic **1** under essentially similar kinetic conditions. The values of F_{IT1}, shown in Table 3, may be compared with F_{IT1} value ($= 0.65$) calculated from eq 4 using data at 0.088 M $C_{16}E_{10}$ summarized in Table S4 (Supporting Information). Thus, these observations suggest that the unexpected large value of A_∞ at 0.088 M $C_{16}E_{10}$ and 1.0×10^{-3} M NaOH is due to near-irreversible micelle-trapped nonreacted **1** molecules.

The irreversible micellar trapping of **1**, as displayed by Figure 4, cannot be entirely explained in terms of the usual shielding effect of micelles where very hydrophobic reactant is buried in the micelles and protected from another very hydrophilic reactant which remains in water. In order to explain the difference between the usual micellar shielding effect and the irreversible micellar trapping described in this manuscript, let us consider the observed kinetic data (k_{obs} vs [$C_{16}E_{10}$]) obtained at 2×10^{-4} M **1**, 1.0×10^{-3} M NaOH, and 35 °C (Table S4, Supporting Information). The values of k_{obs}, obtained within $[C_{16}E_{10}]_T$ range of 5.0×10^{-5} to 3.0×10^{-2} M, followed eq 3 (i.e., the PM model) reasonably well (Figure 3).

The calculated kinetic parameters from eq 3 indicate the fractions of micelle-bound and aqueous-bound **1** as 0.95 and 0.05, respectively, at 0.03 M $C_{16}E_{10}$ while the rate of reaction in the micellar pseudophase is negligible compared to that in aqueous phase. But the value of the fraction of nonreacted micelle-bound **1** (F_{IT1}) is ~0.05 at 0.03 M $C_{16}E_{10}$. However, the value of F_{IT1} becomes ~0.65 at 0.088 M $C_{16}E_{10}$.

The value of the fraction of micelle-bound **1** is >0.98 at 0.088 M $C_{16}E_{10}$. Thus, these results show that ~34% micelle-bound **1** hydrolyzed through the usual equilibrium process $\mathbf{1}_W + D_n \rightleftharpoons \mathbf{1}_M$ assumed in the PM model while ~64% micelle-bound **1** remained nearly irreversibly trapped by micelles. These results can best be represented by Scheme 5 where n_1 $\mathbf{1}_M$ and n_2 $\mathbf{1}_M$ are in equilibrium with n $\mathbf{1}_W$ while n_3 $\mathbf{1}_M$ and n_4 $\mathbf{1}_M$ are not in equilibrium with n $\mathbf{1}_W$. Similarly, s_1 HO^-_M and s_2 HO^-_M ions are in equilibrium with s HO^-_W ions.

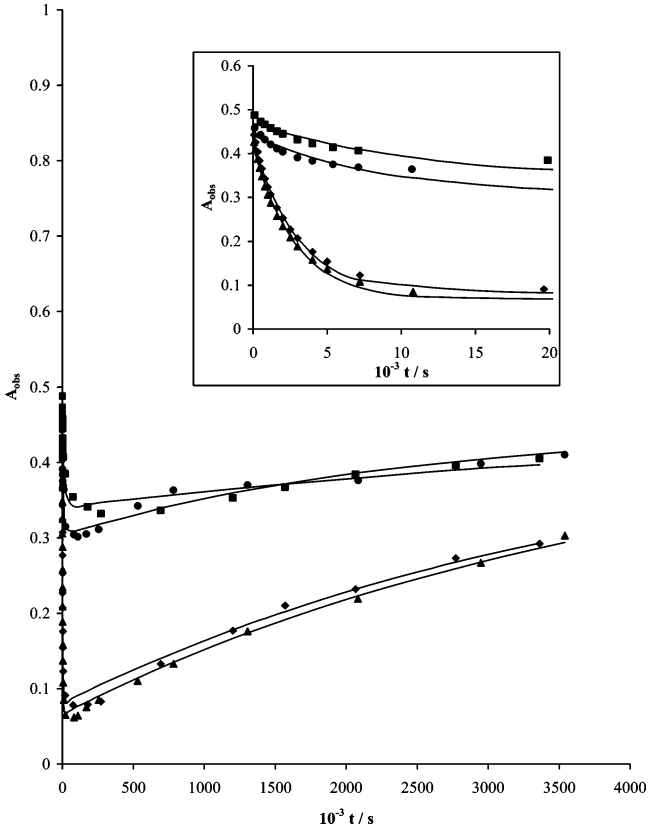

Figure 5. Plots of A_{obs} vs reaction time for hydrolysis of NBPT at 5.0×10^{-2} M {(◆) for first set and (▲) for second set} and 8.8×10^{-2} M {(■) for first set and (●) for second set} $[C_{16}E_{10}]_T$ at 1.0×10^{-3} M NaOH. Solid lines are drawn through the least-squares calculated data points.

Unexpected Minima in the Plots of A_{obs} versus t for $C_{16}E_{10}$-Mediated Alkaline Hydrolysis of 1 Under the Typical Reaction Conditions. The kinetics of the hydrolysis of **1** at 5.0×10^{-2} and 8.8×10^{-2} M $[C_{16}E_{10}]_T$ in the presence of 1.0×10^{-3} M NaOH was complicated by an unexpected increase in the A_{obs} with the increase in reaction time, t, at >21 and 76 h for the reaction rate studied at 5.0×10^{-2} and 8.8×10^{-2} M $[C_{16}E_{10}]_T$, respectively. The representative plots of A_{obs} versus reaction time (t) are shown in Figure 5. These plots show a rapid monotonic decrease in A_{obs} in the initial phase of the reaction followed by a slow monotonic increase with increasing reaction time in the latter phase of the reaction at 300 nm. Similar observations have been reported in the reaction of HO^- with phthalimide in the presence of $\geq 1.2 \times 10^{-2}$ M $C_{12}E_{23}$ in mixed aqueous solvent containing 2% v/v CH_3CN, 2.0×10^{-2} M NaOH, 1.0×10^{-2} M CTABr, and 2.0×10^{-4} M phthalimide.[5] The minima in the plots of Figure 5 demonstrate the formation of a stable intermediate product which absorbs significantly at 300 nm. The most probable such a stable intermediate is phthalic anhydride (**3**) because $\delta_3 \approx 2300$ M^{-1} cm^{-1}, $\delta_2 = \delta_5 = 40$ M^{-1} cm^{-1}, and $\delta_4 = 4$ M^{-1} cm^{-1} at 300 nm where **2**, **4**, and **5** represent *N*-benzylphthalamic acid, benzylamine, and phthalic acid, respectively.

At pH ≤ 3, the rate of N-cyclization (rate constant, $k_{obs} = 1.25 \times 10^{-6}$ s^{-1}) is almost negligible compared to that of O-cyclization (rate constant, $k_{obs} = 17.6 \times 10^{-6}$ s^{-1}) in the

TABLE 4: Values of Kinetic Parameters, k_1, k_2, and A_∞ Calculated from Eq 6[a]

$[C_{16}E_{10}]_T$ M	δ_1^{app} M^{-1} cm^{-1} [b]	δ_3^{app} M^{-1} cm^{-1} [c]	F_{IT1} [d]	$10^5 k_1$ s^{-1}	$10^7 k_2$ s^{-1}	$10^2 A_\infty$	$10^3 \sum d_i^2$ [e]
0.050	1745	2300	0	34.3 ± 1.7[f]	1.88 ± 0.09[f]	8.2 ± 0.4[f]	2.193[g]
	1745	1860	0	34.0 ± 1.7	2.51 ± 0.14	8.1 ± 0.4	2.258
0.050	1750	2300	0	35.5 ± 1.3	1.97 ± 0.08	6.7 ± 0.3	1.633
	1750	1940	0	35.2 ± 1.4	2.49 ± 0.11	6.6 ± 0.3	1.749
0.088	645	800	0.65	8.74 ± 1.70	1.34 ± 0.26	34.1 ± 0.4	2.110[g]
	645	630	0.65	8.76 ± 1.74	1.78 ± 0.38	34.1 ± 0.5	2.169
0.088	687	800	0.65	11.9 ± 1.8	3.27 ± 0.43	30.5 ± 0.4	2.202[h]
	687	730	0.65	11.5 ± 1.7	3.91 ± 0.55	30.4 ± 0.4	2.105
	687	550	0.65	10.6 ± 1.6	7.38 ± 1.42	30.2 ± 0.4	1.867

[a] $[\mathbf{1}_0] = 2.0 \times 10^{-4}$ M, 35 °C, $\lambda = 300$ nm, $[NaOH] = 1.0 \times 10^{-3}$ M. [b] The values of δ_1^{app} were obtained from Table S4 (Supporting Information), where $\delta_{app} = \delta_1^{app}$. [c] $\delta_3^{app} = (1 - F_{IT1})\delta_3^0$ with $\delta_3^0 = 2300$ M^{-1} cm^{-1}. [d] The values of F_{IT1} were calculated from eq 4 with values of A_∞, A_T, A_{T+2}, and A_0 from Table S4 (Supporting Information). [e] $d_i = A_{obs,i} - A_{calcd,i}$ where the values of $A_{calcd,i}$ at the ith reaction time, t_i, were obtained from eq 6 with kinetic parameters listed in Table 4. [f] Error limits are standard deviations. [g] Reaction mixture contained 2% v/v CH_3CN. [h] Reaction mixture contained 0.67% CH_3CN.

cleavage of **2** in aqueous reaction mixture containing 2% v/v CH_3CN.[24] Thus, the aqueous cleavage of **1** follows an irreversible reaction path:

$$\mathbf{1} \xrightarrow{k_1} \mathbf{2} \xrightarrow{k_2} \mathbf{3} + \mathbf{4} \xrightarrow{k_3} \mathbf{4} + \mathbf{5} \qquad (5)$$

The respective absence and presence of a minimum at $[C_{16}E_{10}]_T \leq 3.0 \times 10^{-2}$ M and at $[C_{16}E_{10}]_T \geq 5.0 \times 10^{-2}$ M may be ascribed to the consequence of the effects of $[C_{16}E_{10}]_T$ on the pH of the micellar environment where **2** molecules reside (i.e., $\mathbf{2}_M$ molecules with subscript M representing micellar pseudophase). It is obvious that at $[C_{16}E_{10}]_T \leq 3.0 \times 10^{-2}$ M, the pH of the micellar reaction environment of $\mathbf{2}_M$ remained considerably high and hence the conversion of **2** to **3** in the k_2 step was completely stopped because, in view of related studies,[14,25] anionic *N*-benzylphthalamic acid ($\mathbf{2}^-$) did not undergo O-cyclization to give **3**. However, at $[C_{16}E_{10}]_T \geq 5.0 \times 10^{-2}$ M, the pH of the micellar reaction environment of $\mathbf{2}_M$ dropped to a level where there was significant amount of nonionized $\mathbf{2}_M$ which caused the kinetically detectable occurrence of the conversion of **2** to **3**. An increase in $[C_{16}E_{10}]_T$ at a constant [NaOH] perhaps decreases both $[H_2O]$ and $[HO^-]$ in the micellar region of $\mathbf{2}_M$ molecules, which in turn increases the fraction of nonionized $\mathbf{2}_M$. The increase in the fraction of nonionized $\mathbf{2}_M$ would increase the rate of formation of **3**.

Although the data are not sufficient to carry out a detailed kinetic analysis of the formation of **3**, an attempt was made to fit the observed data at $[C_{16}E_{10}]_T \geq 5.0 \times 10^{-2}$ M (as shown in Figure 5, where there is a maximum change in absorbance in the final phase of the reaction) to eq 6 which is derived from the reaction scheme in eq 5 with the conceivable conditions that $k_3 \ll k_2$ and $\delta_2 \ll \delta_1$ and δ_3 at 300 nm. The assumption that $k_3 \ll k_2$ is based upon the mere observation of increase in A_{obs} with increasing t until the last observed A_{obs} value at $t =$ 983 h. This shows that the water concentration in the micellar environment of reaction $\mathbf{2}_M \rightarrow \mathbf{3}_M + \mathbf{4}_M$, i.e., the k_2 step in eq 5, is extremely low. The plots in Figure 5 should have resulted in maxima if $k_2 \approx k_3$ or $k_2/k_3 \approx 0.5-2.0$ because $\delta_4 + \delta_5$ ($\approx$45 M^{-1} cm^{-1} at 300 nm) $\ll \delta_3$ ($=$ 2300 M^{-1} cm^{-1} at 300 nm). Similarly the plots in Figure 5 should not reveal minima or maxima provided $k_3 \gg k_2$. In eq 6, $[R_0]$ represents the initial concentration of **1** ($= 2.0 \times 10^{-4}$ M), $\delta_1^{app} = \delta_1 - \delta_2$, $\delta_3^{app} = \delta_3 - \delta_2$, and $A_\infty = \delta_2[R_0]$ provided $\delta_4 \approx 0$.

$$A_{obs} = \delta_1^{app}[R_0]\exp(-k_1 t) + \delta_3^{app}[R_0] \times \left\{1 + \frac{1}{k_1 - k_2}[k_2 \exp(-k_1 t) - k_1 \exp(-k_2 t)]\right\} + A_\infty \qquad (6)$$

The nonlinear least-squares fit of the observed data (Figure 5) to eq 6 was carried out by considering k_1, k_2, and A_∞ as unknown parameters at the given values of δ_1^{app} and δ_3^{app}. The mathematical derivation of eq 6 is described in the Supporting Information. The decrease in δ_1^{app} with increase in $[C_{16}E_{10}]_T$ in the initial phase of the plots in Figure 5 is due to nonreacted **1** molecules trapped irreversibly in the micellar region where $[HO^-_M] \approx 0$. The value of δ_1^{app} was obtained from eq 1 (where $\delta_{app} = \delta_1^{app}$) by using the observed data of the fast initial phase of the reaction. The value of δ_3^{app} was obtained from the relationship $\delta_3^{app} = (1 - F_{IT1})\delta_3^0$ where F_{IT1} represents the mole fraction of **1** that remained trapped by micelles in a micellar environment of nearly zero hydroxide ion concentration and δ_3^0 is the molar extinction coefficient of **3** at 300 nm in an aqueous solvent. The values of F_{IT1} at the typical values of $[C_{16}E_{10}]_T$ were calculated from eq 4. The respective values of δ_1 and δ_3 at 300 nm vary from 2250 to 1680 M^{-1} cm^{-1} and 2300−2000 M^{-1} cm^{-1} with increase in acetonitrile content from 2% to 90% in mixed aqueous solvent. However, the values of δ_2 of $\sim$30 M^{-1} cm^{-1} at 300 nm remained unchanged with change in acetonitrile content from 2% to 90% v/v in mixed aqueous solvent containing 0.02 M HCl. An apparent satisfactory fit of observed data to eq 6 is evident from the plots of Figure 5, where solid lines are drawn through the least-squares calculated data points.

The nonlinear least-squares calculated values of k_1, k_2, and A_∞ are shown in Table 4. The values of k_1, k_2, and A_∞ were calculated at different presumed values of δ_3^{app}, because of the uncertainty in the water concentration of micellar reaction environment. However, the results summarized in Table 4 reveal that a significant change in the value of δ_3^{app} caused almost no change in k_1 values and a slight change in $\sum d_i^2$, whereas the value of k_2 was significantly affected. The calculated values of k_1 are similar to the corresponding values of k_{obs} (Table S4, Supporting Information) calculated from eq 1 using A_{obs} values within the reaction time (t) range of 0.02−21 h at 0.050 M $C_{16}E_{10}$ and 0.03−31 as well as 76 h at 0.088 M $C_{16}E_{10}$. The values of k_2 at 0.050 and 0.088 M $C_{16}E_{10}$ are nearly 10^2-fold smaller than the corresponding value of 2.44×10^{-5} s^{-1} obtained in the absence of micelles at 0.02 M HCl and 90% v/v CH_3CN in mixed aqueous solvent.[24] These results may be largely ascribed to the presence of the extremely low value of the fraction of nonionized $\mathbf{2}_M$, $F\{= [\mathbf{2}_M]/([\mathbf{2}_M] + [\mathbf{2}^-_M])$, where $\mathbf{2}^-_M$ represents ionized $\mathbf{2}_M\}$.

Conclusions

It appears that the observed data (A_{obs} vs t) for the rate of alkaline hydrolysis of **1** in the presence of $C_{16}E_{20}$ micelles follow the PM model until a typical value of $R_t = R = [C_{16}E_{20}]_T/[NaOH]$ where the values of $[C_{16}E_{20}]_T$ were varied at a constant value of [NaOH]. The observed data could not follow the PM model at $R > R_t$. Similar observations were obtained in the presence of $C_{16}E_{10}$ micelles. The value of R_t seems to depend upon both the nature of nonionic surfactant and the value of $[C_mE_n]_T/[NaOH]$ ($= R$). The most unusual observation is the sharp decrease in water and hydroxide ion concentrations in the micellar environment of $\mathbf{1}_M$ molecules and consequently irreversible micellar trapping of **1** molecules at $R > R_t$. The alkaline hydrolysis product **2** of **1** is apparently more polar than **1**, and at certain typical values of R for $C_{16}E_{10}$ micelles, the pH of the micellar environment of $\mathbf{2}_M$ became $< \sim 4$ because, under such conditions, $\mathbf{2}_M$ molecules underwent O-cyclization producing **3** as the final stable product. Such observations were not detected in the presence of $C_{16}E_{20}$ micelles although irreversible $C_{16}E_{20}$ micellar trapping of **1** molecules has been detected at certain values of R. Differences in the behaviors of the two surfactants could be most likely related to the differences in the structures. However, the reason related to reactive or higher relative impurity in one of the two surfactants ($C_{16}E_{20}$ and $C_{16}E_{10}$) cannot be completely ruled out.

Acknowledgment. The authors thank the National Scientific Research and Development Council of Malaysia for IRPA (Grant No. 09-02-03-0147), the Academy Sciences Malaysia for SAGA (Grant No. 66-02-03-0039), and the University Malaya for financial assistance.

Supporting Information Available: Tables S1−S4 and mathematical derivation of eq 6 of the manuscript. This material is available free of charge via the Internet at http://pubs.acs.org.

References and Notes

(1) (a) Bunton, C. A. *Catal. Rev.—Sci. Eng.* **1979**, *20*, 1. (b) Bunton, C. A.; Savelli, G. *Adv. Phys. Org. Chem.* **1986**, *22*, 213. (c) Bunton, C. A.; Nome, F.; Quina, F. H.; Romsted, L. S. *Acc. Chem. Res.* **1991**, *24*, 357.

(2) Khan, M. N. Micellar Catalysis. In *Surfactant Science Series*; CRC Press, Taylor & Francis Group: Boca Raton, FL, 2006; vol. 133, p 33 and references therein.

(3) (a) Mishra, A.; Behera, R. K.; Behera, P. K.; Mishra, B. K.; Behera, G. B. *Chem. Rev.* **2000**, *100*, 1973. (b) Mishra, A.; Patel, S.; Behera, R. K.; Mishra, B. K.; Behera, G. B. *Bull. Chem. Soc. Jpn.* **1995**, *70*, 2913. (c) Laschewsky, A. *Curr. Opin. Colloid Interface Sci.* **2003**, *8*, 274. (d) Raghuraman, S.; Pradhan, S. K.; Chattopadhyay, A. *J. Phys. Chem. B* **2004**, *108*, 2489. (e) Sterpone, F.; Pierleoni, C.; Briganti, G.; Marchi, M. *Langmuir* **2004**, *20*, 4311.

(4) Davies, D. M.; Gillitt, N. D.; Paradis, P. M. *J. Chem. Soc., Perkin Trans. 2* **1996**, 659.

(5) Khan, M. N.; Ismail, E. *J. Phys. Org. Chem.* **2002**, *15*, 374.

(6) Khan, M. N.; Ismail, E.; Yusoff, M. R. *J. Phys. Org. Chem.* **2001**, *14*, 669.

(7) Khan, M. N. *J. Chem. Soc., Perkin Trans. 2* **1990**, 445.

(8) Khan, M. N.; Ismail, E. *J. Phys. Org. Chem.* **2004**, *17*, 376.

(9) (a) Khan, M. N.; Ariffin, Z.; Yusoff, M. R.; Ismail, E. *J. Colloid Interface Sci.* **1999**, *220*, 474. (b) Khan, M. N.; Ismail, E. *J. Colloid Interface Sci.* **2001**, *240*, 636.

(10) Cheong, M. Y.; Ariffin, A.; Khan, M. N. *Indian J. Chem.* **2005**, *44A*, 2055.

(11) Khan, M. N. *J. Chem. Soc., Perkin Trans. 2* **1990**, 435.

(12) Broxton, T. J.; Duddy, N. W. *Aust. J. Chem.* **1979**, *32*, 1717.

(13) Bunton, C. A.; Nayak, B.; O'Connor, C. *J. Org. Chem.* **1968**, *33*, 572.

(14) Ariffin, A.; Khan, M. N. *Bull. Korean Chem. Soc.* **2005**, *26*, 1037.

(15) Khan, M. N. *Int. J. Chem. Kinet.* **1987**, *19*, 143.

(16) (a) Menger, F. M.; Portnoy, C. E. *J. Am. Chem. Soc.* **1967**, *89*, 4698. (b) Martinek, K.; Yatsimirskii, A. K.; Levashov, A. V.; Berezin, I. V. In *Micellization, Solubilization, Microemulsion*; Mittal, K. L., Ed.; Plenum: New York, 1977; Vol. 2, p 489.

(17) (a) Bunton, C. A. *Encyclopedia of Surface and Colloid Science*; Hubbert, A. T., Ed.; 2002; p 980. (b) Bunton, C. A. *J. Mol. Liq.* **1997**, *72*, 231. (c) Cordes, E. H.; Gitler, C. *Prog. Bioorg. Chem.* **1973**, *2*, 1. (d) Bunton, C. A. In *Surfactant in Solutions*; Mittal, K. L., Shah, D. O., Eds.; Plenum: New York, 1991; Vol. 11, p 17.

(18) Khan, M. N. Micellar Catalysis. In *Surfactant Science Series*; CRC Press, Taylor & Francis Group: Boca Raton, FL, 2006; vol. 133, pp 215−216.

(19) Broxton, T. J.; Wright, S. *J. Org. Chem.* **1986**, *51*, 2965.

(20) Khan, M. N.; Ariffin, Z. *Langmuir* **1996**, *12*, 261.

(21) Huibers, P. D. T.; Lobanov, V. S.; Katrizky, A. R.; Shah, D. O.; Karelson, M. *Langmuir* **1996**, *12*, 1462.

(22) Rispens, T.; Engberts, J. B. F. N. *J. Org. Chem.* **2003**, *68*, 8520.

(23) Lajis, N. H.; Khan, M. N. *J. Phys. Org. Chem.* **1998**, *11*, 209.

(24) Cheong, M. Y.; Ariffin, A.; Khan, M. N. Submitted for publication.

(25) (a) Hawkins, M. D. *J. Chem. Soc., Perkin Trans. 2* **1976**, 642. (b) Blackburn, R. A. M.; Capon, B.; McRitchie, A. C. *Bioorg. Chem.* **1977**, *6*, 71.